Research Square

Preprints are preliminary reports that have not undergone peer review.
They should not be considered conclusive, used to inform clinical practice,
or referenced by the media as validated information.

Comprehensive Characterization of PEBP Genes Reveals Their Roles in Tuber Development and Stress Responses in Yam

Qiao Qinghua

928401918@qq.com

Yulin Normal University

Gou Ling

Yulin Normal University

Chen Meiling

Yulin Normal University

Sheng Furui

Yulin Normal University

Gao Liujuan

Yulin Normal University

Ren Zhenxin

Yili Normal University

Research Article

Keywords: PEBP gene family, Dioscorea rotundata, Gene expression profiling, Tuber development

Posted Date: September 10th, 2026

DOI: https://doi.org/10.21203/rs.3.rs-9423955/v1

License: This work is licensed under a Creative Commons Attribution 4.0 International License.
Read Full License

Additional Declarations: No competing interests reported.

Comprehensive Characterization of *PEBP* Genes Reveals Their Roles in Tuber Development and Stress Responses in Yam

Qiao Qinghua[1*], Gou Ling[1], Chen Meiling[1], Sheng Furui[1], Gao Liujuan[1], Ren Zhenxin[2*]

1. Key Laboratory of Mountain Biodiversity Conservation, Education Department of Guangxi Zhuang Autonomous Region, Yulin Normal University, Yulin 537000, China;

2. Xinjiang Key Laboratory of Lavender Conservation and Utilization, College of Biological Sciences and Technology, Yili Normal University, Yining 835000, Xinjiang, China;

***Correspondence: Ren Zhenxin, zhxren@126.com; Qiao Qinghua, 928401918@qq.com**

Abstract

The phosphatidylethanolamine-binding protein (PEBP) family regulates flowering, seed development, and underground storage organ formation in plants, yet its functions in yam (*Dioscorea rotundata*) remain unclear. Here, we identified 17 *PEBP* genes in the yam genome and classified them into four clades (FTL, TFL1L, MFTL, and PEBPL). Dispersed duplication was the major driver of gene family expansion, while the limited tandem and segmental duplications evolved under strong purifying selection. Conserved motif and gene structure analyses confirmed the presence of core PEBP domains and indicated subfamily-specific divergence. Promoter analysis revealed abundant light- and hormone-responsive elements, implying complex regulatory inputs. Transcriptome profiling demonstrated distinct tissue-specific expression patterns: *DrPEBP9* and *DrPEBP10* were specifically expressed in flowers, whereas members such as *DrPEBP3*, *DrPEBP15*, *DrPEBP16*, and *DrPEBP17* exhibited tuber-preferential expression. Several *DrPEBP* genes displayed dynamic transcriptional changes during tuber development, indicating potential involvement in tuber expansion and starch accumulation. Additionally, differential expression under scorch foot disease infection and mechanical wounding suggested roles in biotic and abiotic stress responses. Overall, this study provides the first systematic

characterization of the PEBP gene family in yam, highlights candidate genes likely involved in flowering regulation, tuber development, and stress adaptation, and offers valuable resources for future functional studies and genetic improvement of tuber crops.

Keywords: *PEBP* gene family · *Dioscorea rotundata* · Gene expression profiling · Tuber development

Statements and Declarations: The authors declare that the research was conducted in the absence of any commercial, financial, or non-financial relationships that could be construed as a potential conflict of interest.

Key Message

A comprehensive genome-wide analysis of the yam PEBP gene family reveals their evolutionary dynamics, tissue-specific expression, and stage-dependent roles in tuber development and stress responses, and identifies key candidate regulators underlying tuber expansion and environmental adaptation.

Introduction

Phosphatidylethanolamine-binding proteins (PEBPs) are a highly conserved family of proteins found across various biological kingdoms, including plants, animals, and archaea (Danilevskaya et al., 2008). In plants, *PEBP* genes play crucial roles in regulating key developmental processes such as floral transition, flowering time, seed development, dormancy, and tuber formation, making them integral to plant growth and reproduction (Karlgren et al., 2011**;** Bennett et al., 2021; Yu et al., 2019; Yang et al., 2023). The *PEBP* gene family is typically divided into three main subfamilies: Flowering Locus T-like (FT-like), TERMINAL FLOWER 1-like (TFL1-like), and MOTHER OF FT AND TFL1-like (MFT-like) (Hedman et al., 2009; Xu et al., 2022; Wang et al., 2025; Yang et al., 2023).

Over the years, the *PEBP* gene family has been widely identified and studied in several plant species, including *Arabidopsis thaliana* (Li et al., 2022), *Zea mays* (Danilevskaya et al., 2008), *Oryza sativa* (Chardon et al., 2005), *Lycopersicum esculentum* (Zhang et al., 2022), *Triticum* spp (Dong et al., 2020), and others. With the advancement of research, a PEBP-like subfamily has also been identified in some plants (Dong et al., 2020; Fu et al., 2025). These

studies indicate that *PEBP* genes regulate plant growth and development through different mechanisms, including flowering, seed development, and tuber formation. For example, FT-like genes play an important role in promoting flowering in various plants, while TFL1-like genes affect plant reproductive growth by inhibiting or delaying flowering (Ahn et al., 2006；Hanzawa et al., 2005). Additionally, MFT-like genes regulate seed germination, development, and dormancy (Vaistij et al., 2018；Xi et al., 2010)。

In addition to regulating flowering and seed development, *PEBP* genes also play significant roles in the development of underground storage organs. In *Allium cepa* (onion), FT-like genes regulate bulb development through antagonistic interactions with other FT-like genes (Manoharan et al., 2016). In *Solanum tuberosum* (potato), the FT homolog *StSP6A* promotes tuber formation by regulating sucrose transport (Navarro C et al., 2015; Abelenda, et al., 2019; Jing et al., 2023)**.** Furthermore, *StCEN1*, belonging to the TFL1-like subfamily, regulates tuber dormancy release and bud growth (Munevver Dogramaci et al., 2024). The overexpression of *StCEN1* can inhibit tuber formation (Zhang X et al., 2020). In Chrysanthemum, heat stress-induced changes in *PEBP* gene expression may delay flowering and inhibit tuberization (Nakano et al., 2013；Nakano et al., 2020). These findings indicate that *PEBP* genes play a central role in both reproductive growth and the development of underground storage organs such as tubers and bulbs.

Dioscorea spp. (yam) is an important monocot tuber crop with high economic and nutritional value. Yam is rich in starch, sugars, minerals, vitamins, and secondary metabolites such as steroidal saponins and alkaloids, making it an important food and medicinal crop. Globally, yam ranks fourth in root and tuber crop production, following potato (*Solanum tuberosum*), cassava (*Manihot esculenta*), and sweet potato (*Ipomoea batatas*), accounting for about 10% of global root crop production (Viruel J. et al., 2015; Padhan et al., 2020; Khol et al., 2024). The expansion of yam tubers is a key factor in determining its total yield and quality, making the study of tuber development, particularly the regulatory role of *PEBP* genes, crucial for improving yam productivity.

Although the *PEBP* gene family has been widely studied in many plants, its systematic study in yam remains limited. Previous studies have shown that *PEBP* genes play essential roles in flowering, seed development, and the formation of underground storage organs in

plants. Therefore, identifying and characterizing the members of the *PEBP* gene family in yam, and analyzing their expression patterns in different plant tissues, particularly in response to heat stress and during tuber development, is essential for understanding yam's growth and its response to climate change.

This study aims to identify and characterize the *PEBP* gene family members in *Dioscorea rotundata* (yam) through BLASTP searches against the yam genome, and to explore their potential functions in yam growth and development, especially during tuber expansion. The findings of this study are expected to provide new theoretical insights into yam yield and quality improvement and offer a reference for gene regulation research in other tuber crops.

Result

The identification of *PEBP* gene family members in yam

PEBP genes in yam were identified through a bidirectional BLAST strategy and Hidden Markov Model (HMM) analysis, which yielded 17 candidate genes (Table 1). These candidate genes were subsequently validated through comparison with the SwissProt protein database, which confirmed that all 17 candidates were *PEBP* genes. The 17 identified genes were mapped to nine chromosomes in the yam genome (Table 1; Fig 1), based on their chromosomal locations, they were named from *DrPEBP1* to *DrPEBP17*.

Protein parameters of the 17 DrPEBPs were predicted by Protein Parameter Calc. The protein parameters of the 17 DrPEBPs were predicted using the Protein Parameter Calc tool. The DrPEBP proteins consist of 167 to 207 amino acids, with molecular weights ranging from 18.42 to 23.48 kDa. The theoretical isoelectric points (pI) of the proteins vary between 5.21 and 9.16, corresponding to the pH at which the proteins exhibit no net charge (Kozlowski, 2021). The GRAVY values of the DrPEBPs range from -0.517 (DrPEBP12) to 0.008 (DrPEBP8), with the majority of proteins displaying negative values, indicating their predominantly hydrophilic nature. The instability indices for DrPEBP1, DrPEBP17, DrPEBP14, DrPEBP13, and DrPEBP12 are all below 40, suggesting these proteins are relatively stable, whereas the instability indices for the remaining proteins exceed 40. The Aliphatic Index for the DrPEBPs ranges from 72.93 to 88.45. Subcellular localization analysis revealed that four DrPEBPs are localized in the cytoplasm, ten in the nucleus, and three in

120 both the cytoplasm and nucleus (Table 2).

121 **Phylogenetic Relationship Analysis of *DrPEBPs***

122 To investigate the phylogenetic relationships between *DrPEBPs* and their homologous
123 counterparts, a phylogenetic analysis was performed on *DrPEBPs* as well as *Arabidopsis*
124 *PEBPs*. Based on the classification of *PEBPs* in *Arabidopsis*, *DrPEBPs* are grouped into four
125 major clades, which were denoted as FTL, TFL1L, MFTL, and PEBPL clades, comprising 5,
126 5, 2, and 5 members, respectively. Bootstrap values for the *AtPEBPs* and *DrPEBPs* indicated
127 that *DrPEBP15* was the homologous counterpart of *AtATC*, *DrPEBP8* was the homologous
128 counterpart of *AtMFT*. In addition, the phylogenetic proximity between *DrPEBP3*, *DrPEBP6*
129 and *DrPEBP16*, as well as that between *DrPEBP9* and *DrPEBP10*, indicates that these pairs
130 are likely orthologous genes (Fig. 2).

131 **Genome Collinearity Analysis of *DrPEBPs***

132 To unravel the expansion mechanism of the *DrPEBPs*, gene collinearity analysis was
133 performed. Among the 17 *DrPEBPs*, ten were subjected to dispersed duplications, four
134 *DrPEBPs* (*DrPEBP4*/*DrPEBP5* and *DrPEBP13*/*DrPEBP14*) underwent tandem duplication,
135 and two (*DrPEBP3* and *DrPEBP6*) experienced segmental duplication. Additionally,
136 *DrPEBP12* was identified as a singleton.

137 Ka/Ks values of all the tandem and segmental duplication gene pairs were less than 1. The
138 divergence times of the tandem duplication events were 3.35 million years ago
139 (*DrPEBP4*/*DrPEBP5*) and 148.94 million years ago (*DrPEBP13*/*DrPEBP14*). The segmental
140 duplication event occurred 84.92 million years ago.

141 **Gene Structure and Conserved Motifs Analysis of *DrPEBPs***

142 To examine the structural characteristics of *DrPEBPs*, we analyzed the gene structures and
143 conserved motifs of DrPEBPs. An unrooted phylogenetic tree that combines the motifs was
144 constructed based on the full lengths of the 17 *DrPEBP* gene sequences by using the
145 Maximum-Likelihood method, as illustrated in Fig. 4.

146 The majority of *DrPEBPs* contained four exons (11/17), followed by five exons (3/17).
147 *DrPEBP4* and *DrPEBP5* each contained three exons, while *DrPEBP12* contained two exons.
148 All DrPEBPs included a PEBP superfamily domain (Supplementary Fig. 1).

149 The MEME Suite Wrapper of TBtools software was used to identify the conserved protein

motifs, with a maximum number of the different motifs at 10. A total of 7 conserved motifs were identified across the DrPEBP proteins. Except for DrPEBP12, Motifs 1, 2, 3, 4, and 5 are conserved in all DrPEBP members, arranged in the pattern Motif 3-Motif 5-Motif 1-Motif 4-Motif 2. DrPEBP12 contains only Motif 1 and Motif 4. Motifs 6 and 7 are present only in certain members of the PEBPL subfamily.

To further investigate the structural and functional conservation of these proteins, amino acid sequence alignment was performed for DrPEBP proteins. The results revealed 14 conserved amino acid residues across the DrPEBP protein sequences. Except for DrPEBP1 and DrPEBP12, all other DrPEBP proteins contained the DPDxP motif, a hallmark of the PEBP family. In addition, all DrPEBP proteins, except DrPEBP12, possessed the GxHR motif, another key functional domain. We also observed several relatively conserved amino acid residues within the subfamilies. For example, at position 140, the majority of DrPEBP proteins, except for the two MFTL members, contained aspartic acid (D), while MFTL members had asparagine (N) at this position. At position 127, all five PEBPL members had asparagine (N), while all five TFL1L members contained aspartic acid (D). At position 133, all five TFL1L members had histidine (H), the two MFTL members had tryptophan (W), and the other members predominantly contained tyrosine (Y). At position 143, all five PEBPL members contained glutamic acid (E), while all five TFL1L members had glycine (G) at this position.

Analysis of Cis-acting Elements in Promoters of *DrPEBPs*

Cis-acting elements are critical for regulating gene transcription. In this study, we analyzed the 2000 bp upstream sequences of the *DrPEBP* of the translation initiation sites to predict and characterize cis-acting elements (Figure 6). In addition to the core promoter elements, we identified 42 cis-acting elements involved in 17 biological processes. These processes are classified into five major categories: Environment (26 cis-acting elements), Phytohormone (8 cis-acting elements), Stage (1 cis-acting elements), TF (MYB-binding，3 cis-acting elements), and Tissue (4 cis-acting elements). Among these elements, light-responsive elements were the most abundant. In the 17 *DrPEBPs*, 21 types of light responsiveness-related elements were identified, totaling 213 instances. Notably, *DrPEBP12* and *DrPEBP14* contained 23 and 22 light responsiveness-related elements, respectively. The second most prevalent elements were

abscisic acid responsiveness-related elements (ABRE), with 39 ABRE elements detected across the 17 *DrPEBPs*. These elements were most abundant in *DrPEBP12* and *DrPEBP14*, each containing 7 ABRE elements, followed by *DrPEBP8* (5 elements). In contrast, development-related elements were the least frequent. In addition to ABA-responsive elements, several other hormone-responsive elements were identified, including those related to gibberellin, MeJA, salicylic acid, auxin, and zein. Furthermore, elements associated with low-temperature, defense and stress, and drought responses were also detected. Detailed information on the cis-acting elements in the promoter regions of *DrPEBP* genes is provided in Supplementary Table S1.

Expression Profiles of *DrPEBPs* in Different Tissues of Yam

To investigate tissue-specific gene expression patterns across various tissues, the expression of *DrPEBPs* was examined using RNA-seq data (DRP003729). It was shown that *DrPEBP5* and *DrPEBP7* exhibit consistently high expression levels across all tissues. *DrPEBP9* and *DrPEBP10* are specifically expressed in flower organs, whereas *DrPEBP3*, *DrPEBP15*, *DrPEBP16*, and *DrPEBP17* are specifically expressed in yam tubers. *DrPEBP13* shows elevated expression in yam roots, leaves, and tubers. Notably, four TFL (*DrPEBP9*, *DrPEBP10*, *DrPEBP11*, *DrPEBP14*), two TFL1L (*DrPEBP2*, *DrPEBP6*, *DrPEBP11*, *DrPEBP14*) , and all MFTL (*DrPEBP8*, *DrPEBP12*) subfamily members are not expressed in yam tubers (Fig 7A; Supplementary Table S2).

Expression Analysis of the *DrPEBP*s During the Development of Tuber in Yam

To explore the potential role of *DrPEBPs* in tuber expansion and starch synthesis, we analyzed its expression levels in yam tubers at different developmental stages, utilizing transcriptome data from the NCBI SRA database (SRP186810). The results indicated that the expression levels of four FTL subfamily genes (*DrPEBP10*, *DrPEBP9*, *DrPEBP11*, *DrPEBP14*), two MFTL subfamily genes (*DrPEBP8*, *DrPEBP12*), and two TFL1L subfamily genes (*DrPEBP2*, *DrPEBP6*) were extremely low (<1) or nearly undetectable throughout the entire developmental process of yam tubers. During yam tuber development, the expression levels of *DrPEBP3*, *DrPEBP13*, *DrPEBP16*, and *DrPEBP17* initially decrease and then increase. These genes show a significant decline from the initiation to the early stage, followed by a sharp increase from the early to the middle stage, reaching their peak

expression levels in the middle stage. Notably, the expression level of *DrPEBP13* in the middle stage is 11.11 times higher than in the early stage. In contrast, the expression levels of *DrPEBP1*, *DrPEBP4*, *DrPEBP5*, and *DrPEBP15* gradually decrease throughout tuber development, reaching their lowest levels at the middle stage. Subsequently, their expression levels gradually rise as the tubers transition from the middle to the mature stage (Fig 7B).

The expression levels of *DrPEBP* genes during tuber expansion were further validated through analysis of transcriptome data from the NCBI SRA database (SRP152752). The SRP152752 transcriptome data also revealed no expression of the eight genes that were previously undetected in the tuber. Furthermore, the expression levels of *DrPEBP1*, *DrPEBP3*, *DrPEBP5*, *DrPEBP13*, *DrPEBP16*, and *DrPEBP17* showed considerable variation across different developmental stages of the tuber (Fig 7B; Supplementary Fig 2; Supplementary Table S3).

Based on the result before, four PEBPL members (*DrPEBP1*, *DrPEBP4*, *DrPEBP5*, and *DrPEBP17*), one FTL member (*DrPEBP13*), and three TFL1L members (*DrPEBP15*, *DrPEBP16*, and *DrPEBP3*) were selected for qRT-PCR validation. As shown in Fig. 8, *DrPEBP4*, *DrPEBP5*, and *DrPEBP13* reached peak expression levels at the early stage of tuber expansion (60 days after planting), whereas *DrPEBP1*, *DrPEBP3*, and *DrPEBP17* exhibited the highest expression levels at the late stage of tuber expansion (150 days after planting). In contrast, the expression levels of *DrPEBP15* and *DrPEBP16* gradually decreased during tuber expansion and reached their lowest levels at the late stage (150 days after planting). These results indicate that the expression patterns of these genes are significantly influenced by tuber developmental stages.

Expression profiles of *DrPEBPs* in Response to Biotic and Abiotic Stresses

To investigate the expression of *DrPEBPs* in yam tubers affected by scorch foot disease, we analyzed transcriptomic data from mature tubers of both healthy and end black disease-infected yams, and characterized the expression profiles of these genes. The results indicated that, compared to healthy tubers, the expression levels of *DrPEBP2*, *DrPEBP4*, *DrPEBP12*, and *DrPEBP16* in the diseased tubers showed significant differences. Specifically, the expression of *DrPEBP2*, *DrPEBP4*, and *DrPEBP12* was significantly increased by 2.57, 1.40, and 3.70-fold, respectively, while the expression of *DrPEBP16* was

significantly down-regulated (Fig 9A; Supplementary Table S4).

The expression profiles of *DrPEBPs* in yam tubers subjected to mechanical injury were analyzed using RNA-seq data from tubers at 0 and 3 days post-injury. The expression levels of *DrPEBP1*, *DrPEBP5*, and *DrPEBP13* in yam tubers at 3 days post-injury were significantly reduced compared to day 0, with expression levels at 0.11, 0.45, and 0.16 times those at day 0, respectively (Fig 9B; Supplementary Table S5).

Discussion

Identification of the *DrPEBP* Gene Family in Yam

The PEBP family is widely distributed across plant species, and in recent years, *PEBP* gene family were identified in a variety of plants. Extensive research has demonstrated that *PEBP* genes play pivotal roles in plant growth and development, including the regulation of flowering in *Arabidopsis* and rice (Jeong et al., 2005; Vaistij et al., 2013; Sun et al., 2012; Komiya et al., 2008), seed germination in plants such as cotton (Yu et al., 2019), and the formation of underground storage organs like potato tubers (Navarro et al., 2011; Abelenda et al., 2016; Morris et al., 2018; Zhang et al., 2020), as well as sweet potato and onion bulbs (Lee et al., 2013). Similar to potato tubers and onion bulbs, the yam's main edible organ, the tuberous root, is also an underground storage organ. Therefore, investigating the PEBP family members in yam could significantly contribute to improving tuber yield. Despite extensive research on the PEBP family in other plant species, its function in yam remains insufficiently explored. Therefore, there is a pressing need for further investigation into the function of the *DrPEBP* family in yam.

In this study, we identified 17 *DrPEBP* genes from the complete yam genome sequences. The number of *DrPEBP* genes in yam is comparable to that in *Solanum tuberosum* (15) (Zhang et al., 2022), *Hedychium coronarium* (14) (Wang et al., 2025), and *Solanum lycopersicum* (12) (Sun et al., 2023), and approximately three times that in *Castanea mollissima* (6) (Tian et al., 2025). This discrepancy may be attributed to the distinct selective pressures experienced by different species during evolution, leading to variations in gene expansion patterns. The identified genes exhibit diverse lengths, encoding proteins ranging from 167 to 207 amino acids, with molecular weights ranging from 18.42 to 23.48 kDa. These

genes are distributed across seven chromosomes and two unanchored scaffolds. Their physicochemical properties, including isoelectric points (pI), range from 5.21 to 9.16, suggesting the broad functional diversity of these genes.

Traditionally, *PEBP* genes are classified into three main clades: MOTHER OF FT AND TFL1 (MFT), FLOWERING LOCUS T (FT), and TERMINAL FLOWER 1 (TFL). In addition, a PEBPL subfamily has been identified in several plant species, including *Solanum tuberosum*, wheat, and cotton (Zhang et al., 2022; Dong et al., 2020; Zhang et al., 2016). In this study, phylogenetic analysis revealed that the *DrPEBP* gene family in yam consists of four subfamilies: FTL, TFL1L, MFTL, and PEBPL. Previous studies have shown that the distribution of PEBP family members across subfamilies is uneven. In *Ananas comosus* (pineapple), the FTL subfamily contains the largest number of members (7/11) (Zhang et al., 2023). Similarly, in *Hedychium coronarium*, the FTL subfamily is the largest (9/14), followed by TFL1L (4/14), with the MFTL subfamily being the smallest (1/14) (Wang et al., 2025). In yam, the *DrPEBP* gene family members are more evenly distributed across the FTL, TFL1L, and PEBPL subfamilies, each containing five members. However, the MFTL subfamily is represented by only two members, which aligns with previous findings.

Most *DrPEBP* Genes Underwent Dispersed Duplication

Gene duplication events are prevalent in plant genomes and play a crucial role in driving plant evolution (Bowers et al. 2003). Members of a gene family originate from a common ancestor and evolve through processes such as mutation, domestication, and selection, ultimately forming a group of genes that encode similar proteins with comparable sequences and structures. Gene duplication events can be classified into single-gene duplication and whole-genome duplication (WGD). Genes generated through WGD often undergo loss or silencing over time, leading to a rapid return to a diploid state in plants (Lynch et al. 2000). In contrast, single-gene duplication can occur through several mechanisms, including tandem duplication, proximate duplication, dispersed duplication, and separated duplication (Qiao et al. 2019). These gene duplication events enhance the evolutionary efficiency of plants, providing them with greater adaptability to various environmental conditions. Previous studies of the PEBP family in pineapple demonstrated that *PEBP* genes mainly arose by segmental duplication (Zhang et al. 2023). In *Castanea mollissima*, the expansion of the

CmPEBP genes was mainly driven by dispersed duplication (Tian et al. 2025). In this study, intraspecific collinearity analysis showed that most of *DrPEBPs* were subjected to dispersed duplications, only the *DrPEBP*3 and *DrPEBP*6 genes had collinearity, indicating that *DrPEBP* gene family members had fewer copies, or that their copies were discarded more during evolution.

The ratio of nonsynonymous (Ka) to synonymous (Ks) substitutions is a key parameter for evolutionary analysis (Cao et al., 2016b). In our study, the Ka/Ks values for all tandem and segmental duplication gene pairs were less than 0.3, suggesting that these *DrPEBP* gene pairs might have experienced strong purifying selection during their evolution. The divergence time of duplication events revealed that the tandem duplication between the *DrPEBP13* and *DrPEBP14* gene pairs occurred approximately 100 to 200 million years ago (MYA), indicating that these duplications took place during the divergence between monocots and dicots (100-200 MYA) (Vision et al., 2000; Wang et al., 2005). In contrast, the tandem duplication event between *DrPEBP4* and *DrPEBP5* occurred around 3 million years ago, while the segmental duplication event between *DrPEBP3* and *DrPEBP6* took place approximately 80 million years ago. These findings suggest that the *DrPEBP* gene family in yam may have undergone a prolonged evolutionary history; however, during this extended evolution, it likely encountered strong selective pressures that limited the expansion of its gene family members.

Gene Structure and Motif Analysis Reveal the Key Role of *DrPEBPs* in Growth Regulation

Gene structure has been shown to influence gene function by affecting RNA splicing, RNA stability, and chromatin organization (Carle-Urioste et al., 1997; Mattick and Gagen, 2001; Schwartz et al., 2009). Genes with multiple introns provide opportunities for alternative splicing, thereby enhancing protein functional diversity at the post-transcriptional level (Xiang et al., 2015). In this study, both the FTL and TFL1 subfamilies consist of four exons and exhibit a similar distribution of conserved motifs, indicating that these genes are evolutionarily conserved. However, in contrast to the FTL and TFL1L subfamilies, the *DrPEBP1*, *DrPEBP7*, *DrPEBP17* genes contain five introns, while *DrPEBP12* has only two introns. The acquisition and loss of exons and introns, along with significant changes in

conserved patterns within the MFTL and PEBPL subfamilies in pineapple, suggest the existence of functional diversity between the MFTL and PEBPL subfamilies.

DrPEBPs Might Play Multiple Functions in Different Tissues

The *PEBP* gene family members are essential in regulating various processes, including flowering, seed development, dormancy, and plant morphogenesis (He et al., 2022; Kaneko-Suzuki et al., 2018; Kim et al. 2022; Wang et al., 2025). Research in other plant species has shown that members of the FTL subfamily play significant roles in plant development. For instance, four FT-like genes in *Solanum lycopersicum*, namely *SlSP5G*, *SlSP5G2*, *SlSP5G3*, and *SlSP3D*, are involved in the photoperiodic regulation of tomato flowering (Cao et al., 2016a). Additionally, the overexpression of *FtFT1* and *FtFT3* genes has been shown to promote flowering and increase yield in *Fagopyrum tataricum* (Nie et al., 2024). In *Eriobotrya japonica*, EjFT1 and EjFT2 regulate flower bud differentiation by competitively binding to EjFD (Jiang et al., 2025). In yam, we identified two FTL members (*DrPEBP9* and *DrPEBP10*) that are specifically expressed in flower organs, suggesting that these genes may play a role in regulating reproductive transformation and the progression of flowering. In *Arabidopsi*s, the PEBP homologs AtFT and AtTFL1 are key regulators of flowering, with opposing roles: AtFT promotes flowering, while AtTFL1 inhibits it. Overexpression of *AtTFL1* in shoot apical meristems has been shown to extend both the vegetative and floral phases (Fernández-Nohales et al., 2014). Our findings also reveal that three TFL1L subfamily members, *DrPEBP3*, *DrPEBP15*, *DrPEBP16*, and a PEBPL subfamily member (*DrPEBP17*) are specifically expressed in yam tubers. During yam tuber development, the expression levels of the three TFL1L subfamily members exhibit significant changes, either increasing or decreasing, highlighting their crucial regulatory roles in tuber development. Interestingly, two PEBPL subfamily members, *DrPEBP5* and *DrPEBP7*, exhibit consistently high expression levels across all tissues, indicating their potential involvement in broad regulatory processes related to plant growth and development. As tuber development progresses, the expression levels of *DrPEBP1*, *DrPEBP4*, and *DrPEBP5* in the tuber exhibit significant stage-specific variations, with a pattern similar to that of the TFL1L subfamily member DrPEBP15.

Expression Analysis Revealed _DrPEBPs_ Respond to Biotic and Abiotic Stresses

In addition to their roles in regulating vegetative and reproductive growth, PEBP genes have been implicated in the response to both biotic and abiotic stresses. For instance, *TaPEBP1*, *TaPEBP3*, and *TaPEBP5* are critical for the response of *Triticum aestivum* to drought, cold, and heat stress (Dong et al., 2020). Tian et al. (2025) demonstrated that *CmPEBP* plays a pivotal role in the plant response to temperature stress, drought, and infestation by the gall wasp (*Dryocosmus kuriphilus*, GWDK). In *Solanum tuberosum*, FT and TFL1 family members have been shown to mediate heat stress responses in leaves, roots, and tubers (Zhang et al., 2022). In the present study, the expression of *DrPEBP2*, *DrPEBP4*, *DrPEBP12*, and *DrPEBP16* in yam tubers indicates their potential involvement in disease resistance mechanisms. Moreover, *DrPEBP1*, *DrPEBP5*, and *DrPEBP13* appear to play significant roles in the repair processes of wounded yam tubers.

Material and method

Identification of *PEBP* Genes in Yam

PEBP genes of *Arabidopsis thaliana* were retrieved from GenBank and The Arabidopsis Information Resource (TAIR). The genomic data and gene annotations for *Dioscorea rotundata* data were sourced from Phytozome. A local BLAST search was performed using TBtools (v1.108) to identify potential *DrPEBP* genes, using *Arabidopsis PEBP* gene sequences as queries. The E-value threshold was set to 1e-5, and a maximum of 500 sequences were retrieved in the initial search, with 250 sequences selected for final alignment. The initial round of analysis identified 17 candidate sequences, which were then further analyzed through BLAST searches against the SwissProt protein database (https://www.uniprot.org/uniprotkb?query=reviewed:true). These 17 sequences were classified as *DrPEBP* genes (Table 1).

Chromosomal Location and Collinearity Analysis of *DrPEBP* Genes

Genomic localization information for the *DrPEBP* genes were obtained from the Phytozome database. The data were filtered using TBtools, and the chromosomal distribution of the genes was visualized using the Advanced Circos module in TBtools. Collinearity analysis of the *DrPEBP* genes was conducted using MCScanX in TBtools, applying the default settings.

Characteristics of DrPEBP Proteins

The molecular weight (Da) and isoelectric point (pI) of the DrPEBP proteins were determined

using the Protein Parameter Calc (TBtools-II) tool based on the full-length proteins.

Phylogenetic Analysis of DrPEBP Proteins in Yam

The DrPEBP protein sequences from yam and *Arabidopsis thaliana* were aligned using ClustalW in MEGA 11.0.13 with default parameters. The optimal substitution model was selected in MEGA 11.0.13, and the tree was generated using the maximum-likelihood method with the JTT+G model and 1,000 bootstrap iterations. iTOL v6 (https://itol.embl.de/) was used to visualize the tree.

Promoter Cis-regulatory Element Analysis

A 2000 bp fragment upstream of the *DrPEBP* coding region was extracted as the promoter region. Cis-regulatory elements in the *DrPEBP* promoters were identified using the PlantCARE database (https://bioinformatics.psb.ugent.be/webtools/plantcare/html/). Cis-elements potentially associated with key biological processes were retained. Further details are provided in Supplementary Table S1. TBtools (Simple Biosequence Viewer) was used to visualize the cis-elements, which ensured that the regulatory sequences were comprehensively analyzed.

Gene Expression Analysis

Transcriptome data for *DrPEBP* genes from different tissues and treatments in yam were obtained from the Sequence Read Archive (SRA) database with the following accession numbers: DRP003729, SRP186810, SRP152752, SRP298405, and SRP445455. Specifically, DRP003729 provides tissue-specific gene expression patterns, SRP186810 and SRP152752 include expression levels of yam tubers at different developmental stages, SRP298405 contains data for tuber of both yam scorch foot disease and healthy samples, and SRP445455 includes data from tuber samples collected at two different time points (0 days and 3 days) post-wounding. These transcriptome datasets were downloaded and converted to FASTQ format. Transcript abundance was quantified using the Kallisto Super GUI Wrapper (TBtools-II) and a pseudo-alignment algorithm. The raw reads were pseudo-aligned to the yam reference transcriptome, and their expression values were normalized to transcripts per million (TPM). Next, the normalized data were extracted, log2-transformed, and visualized via a heatmap generated with Table Row Extract or Filter (TBtools-II).

Quantitative Real-time PCR (qRT-PCR) Validation

The sampling of yam tubers across different developmental stages and the qRT-PCR assays were conducted as previously described (Qiao et al., 2025), without modification.

Full-length coding sequence of rna-XM_039266833.1 (DrPEBP1), rna-XM_039269827.1 (DrPEBP3), rna-XM_039272669.1 (DrPEBP4), rna-XM_039272711.1 (DrPEBP5), rna-XM_039280148.1 (DrPEBP13), rna-XM_039283695.1 (DrPEBP15), rna-XM_039260562.1 (DrPEBP16), rna-XM_039260561.1 (DrPEBP17) were retrieved from the yam genome database for primer design. Gene-specific primers were designed using Primer Premier 5 and validated for specificity using NCBI BLAST (https://blast.ncbi.nlm.nih.gov/Blast.cgi?PROGRAM=blastn&PAGE_TYPE=BlastSearch&LINK_LOC=blasthome). *DrACTIN* was used as the reference gene. Primers sequences are provided in Supplementary File: Table S6. qRT-PCR was performed using ArtiCanATM SYBR qPCR Mix (Tsingke, Beijing, China). Three independent biological replicates were included for each sample. Relative expression levels of *DrPEBPs* were calculated using the $2^{-\Delta\Delta CT}$ method.

Figures and Tables

Table 1 Information on the 17 identified *DrPEBP* genes in yam.

GeneID	rename	Chr ID	Gene Range	mRNA ID	Num of Exon
gene-LOC120259259	DrPEBP1	NC_052474.1	21221008:21222441	rna-XM_039266833.1	5
gene-LOC120259234	DrPEBP2	NC_052474.1	4099722:4100773	rna-XM_039266807.1	4
gene-LOC120261831	DrPEBP3	NC_052475.1	709629:710866	rna-XM_039269827.1	4
gene-LOC120261716	DrPEBP4	NC_052475.1	2024180:2025785	rna-XM_039269698.1	3
gene-LOC120261049	DrPEBP5	NC_052475.1	1999657:2001262	rna-XM_039268718.1	3

gene-LOC120270732	DrPEBP6	NC_052480.1	446217:447220	rna-XM_039277805.1	4
gene-LOC120270900	DrPEBP7	NC_052480.1	2012901:2014540	rna-XM_039277973.1	5
gene-LOC120280933	DrPEBP8	NC_052487.1	1432947:1434165	rna-XM_039287903.1	4
gene-LOC120281358	DrPEBP9	NC_052487.1	7343725:7344913	rna-XM_039288202.1	4
gene-LOC120280039	DrPEBP10	NC_052487.1	8245761:8246921	rna-XM_039286737.1	4
gene-LOC120280669	DrPEBP11	NC_052487.1	18293144:18294841	rna-XM_039287585.1	4
gene-LOC120282702	DrPEBP12	NC_052488.1	21971571:21972331	rna-XM_039289554.1	2
gene-LOC120251086	DrPEBP13	NC_052490.1	30754797:30756925	rna-XM_039259625.1	4
gene-LOC120251067	DrPEBP14	NC_052490.1	30773232:30776925	rna-XM_039259609.1	4
gene-LOC120253156	DrPEBP15	NC_052496.1	2276:3385	rna-XM_039261469.1	4
gene-LOC120253832	DrPEBP16	NW_024086611.1	48860:49803	rna-XM_039262049.1	4
gene-LOC120256890	DrPEBP17	NW_024088090.1	48879:53620	rna-XM_039264560.1	5

Table 2 Protein parameters of the 17 DrPEBPs.

rename	Number of Amino Acid	Molecular Weight	Theoretical pI	Instability Index	Aliphatic Index	Grand Average of Hydropathicity	Subcellular localization

DrPEBP3	174	19737.53	8.6	41.96	81.15	-0.318	Cytoplasm
DrPEBP6	173	19570.47	9.16	41.73	86.13	-0.203	Cytoplasm.
DrPEBP11	177	19672.46	9.12	47.11	88.08	-0.215	Cytoplasm.
DrPEBP16	189	21428.55	8.02	40.55	88.15	-0.257	Cytoplasm.
DrPEBP2	173	19497.14	7.07	43.12	79.88	-0.402	Cytoplasm. Nucleus
DrPEBP15	174	20181.23	8.17	42.58	83.91	-0.302	Cytoplasm. Nucleus
DrPEBP8	172	18705.59	7.77	55.32	78.02	0.008	Cytoplasm. Nucleus.
DrPEBP1	178	20038.62	6.07	31.15	77.58	-0.33	Nucleus
DrPEBP4	207	23482.88	7.62	47.63	87.54	-0.201	Nucleus
DrPEBP5	207	23392.8	7.62	40.65	88.45	-0.181	Nucleus
DrPEBP7	184	20905.66	6.42	43.7	76.74	-0.377	Nucleus
DrPEBP9	184	20749.49	5.92	48.37	78.8	-0.184	Nucleus
DrPEBP10	176	19814.41	6.73	41.42	77.44	-0.32	Nucleus
DrPEBP12	167	18417.93	5.21	38.43	72.93	-0.517	Nucleus
DrPEBP13	177	20101.81	7.84	35.53	77.06	-0.275	Nucleus
DrPEBP17	175	19896.51	5.59	33.54	82.86	-0.309	Nucleus
DrPEBP14	175	19583.28	9.06	35.1	78.97	-0.232	Nucleus.

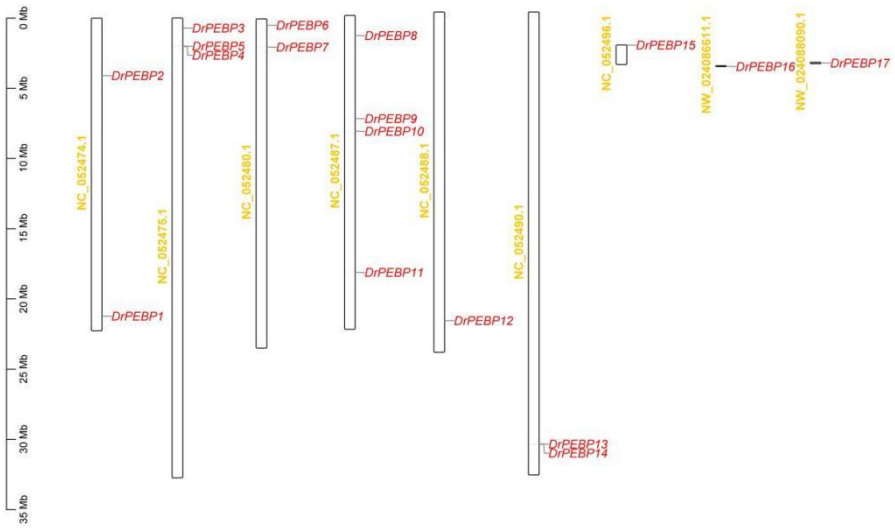


Fig. 1 Chromosomal mapping of *DrPEBPs* in the yam genome. 15 *DrPEBP* genes (*DrPEBP1-DrPEBP15*) were distributed across chromosomes with NC identifiers, *DrPEBP16* and *DrPEBP17* was located on an unanchored scaffold labeled with an NW identifier. The chromosomal positions were visualized using TBtools. The scale on the left indicates chromosome length in megabases (Mb). Chromosomes without *DrPEBP* genes are

not shown.

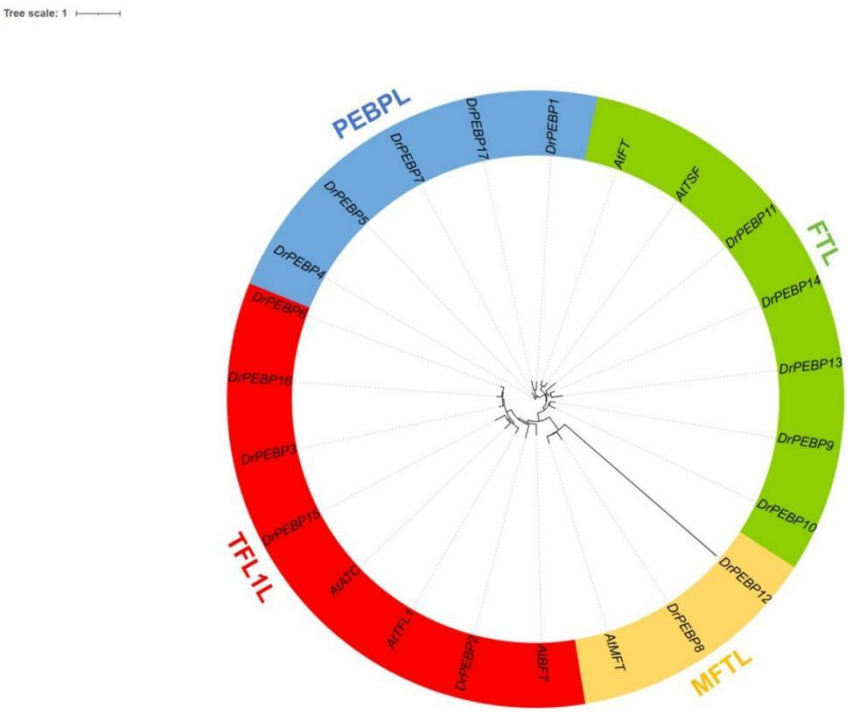


Fig. 2 Phylogenetic tree of *PEBP* gene family members in yam and *Arabidopsis*. Based on the classification of *PEBP* gene family members in *Arabidopsis*, *DrPEBP* are grouped into four major clades, represented by red, yellow, green, and blue.

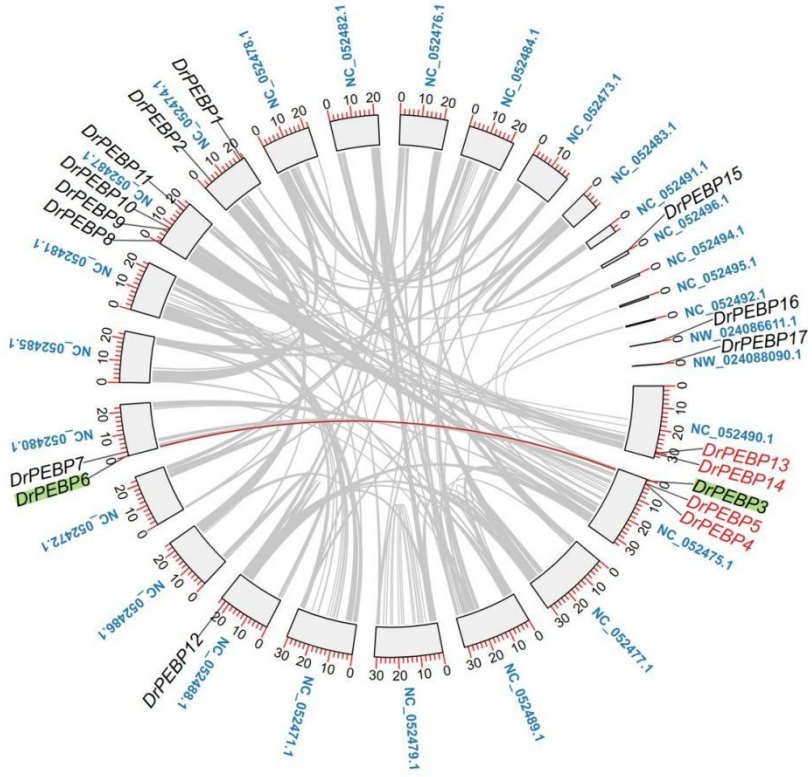


Fig. 3 Duplication analysis of DrPEBPs. In the center, gray lines represent synteny blocks in the *Dioscorea rotundata* genome, and red lines between chromosomes mark segmental duplication gene pairs. The rectangle on the outer ring represent yam chromosomes. Gene names with the same back color (green) represent segmental duplication gene pairs. Gene names in the same color (red) represents tandem duplication gene pairs.

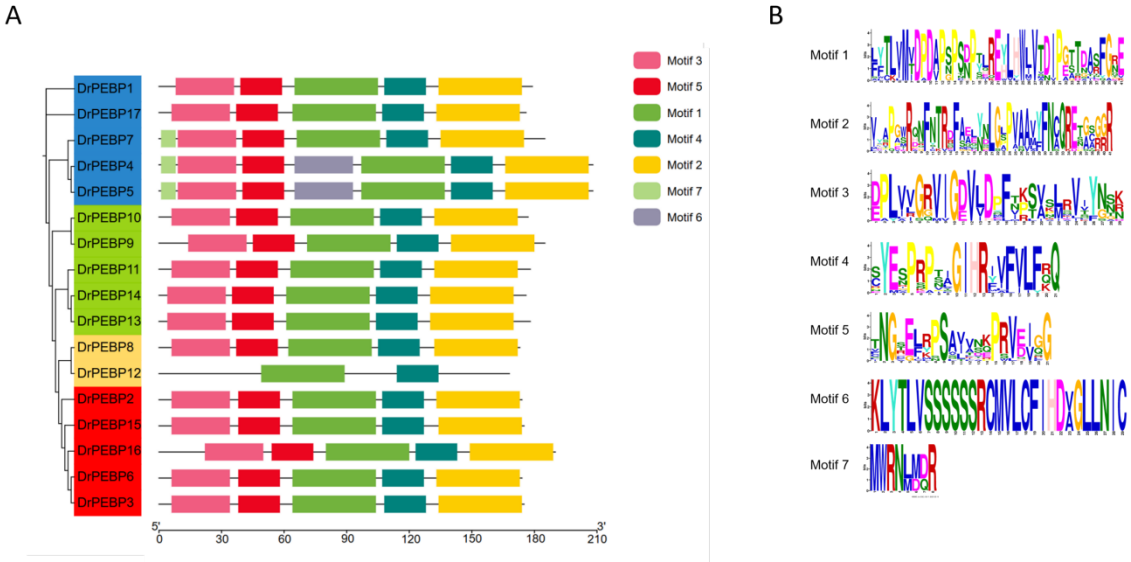
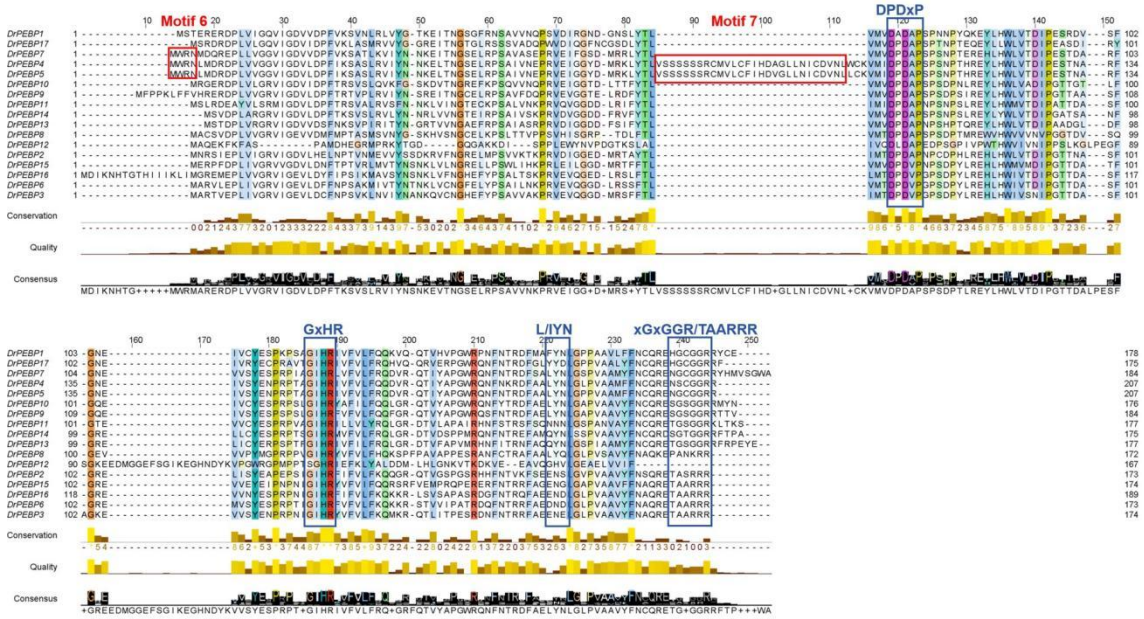


Fig. 4 Conserved domain analysis of the DrPEBPs. (A) Phylogenetic relationships and conserved motifs of DrPEBPs; (B) Conserved motif logos constituting the DrPEBP domain.



459

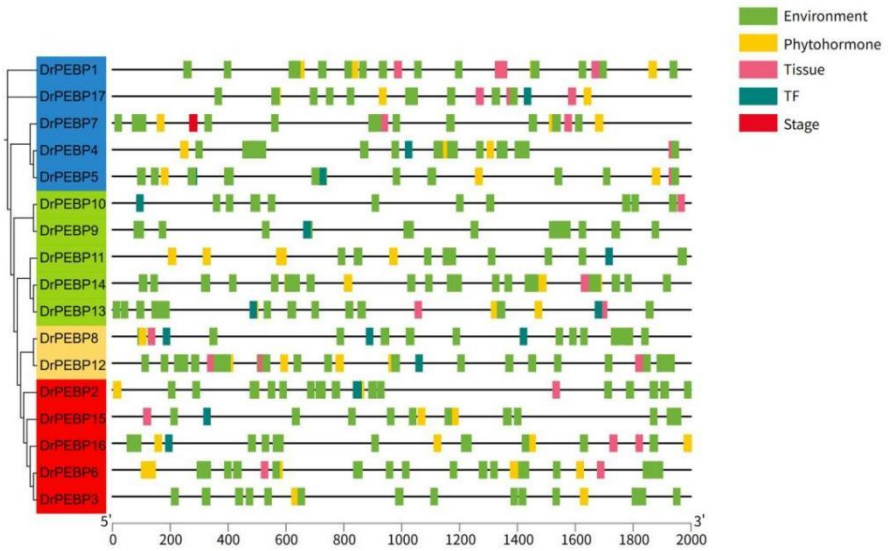
460

461 **Fig. 5 Multiple sequence alignment of DrPEBP proteins.** Conservation: The conservation

462 of the total alignment, with less than 25% gaps; Quality: Alignment quality based on

463 Blosum62 scores.

464 **A**



465

466 **B**

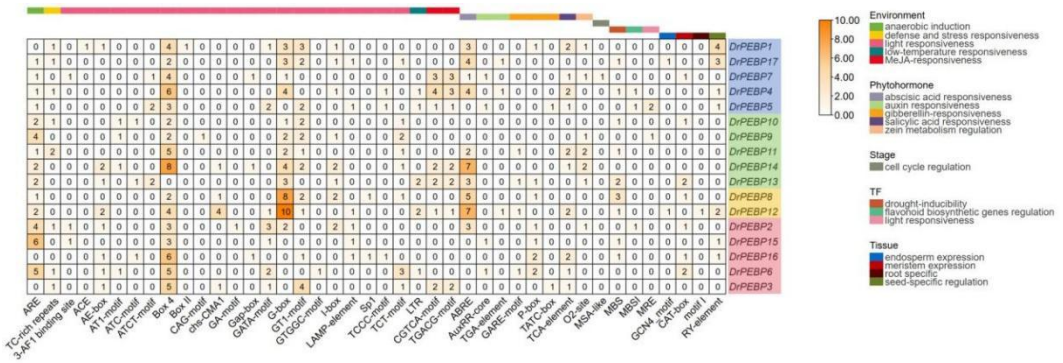
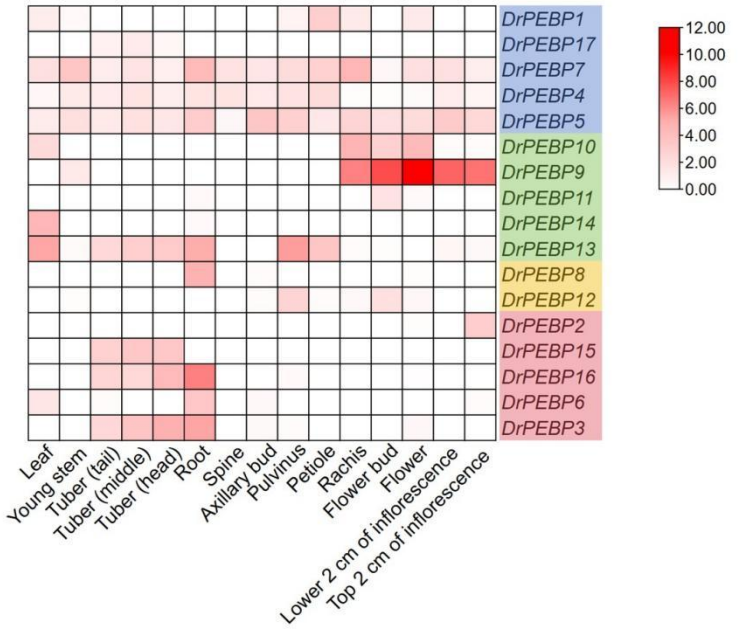


Fig. 6 Cis-acting elements analysis in the promoter sequences of *DrPEBPs*. (A) Distribution of cis-acting elements in the 2000 bp upstream promoter regions of *DrPEBPs*. Different colors represent various element types. A ruler indicates sequence direction and length. (B) Classification and statistics heatmap of cis-acting elements. Numbers and colors indicate the count of specific elements per gene.

A



B

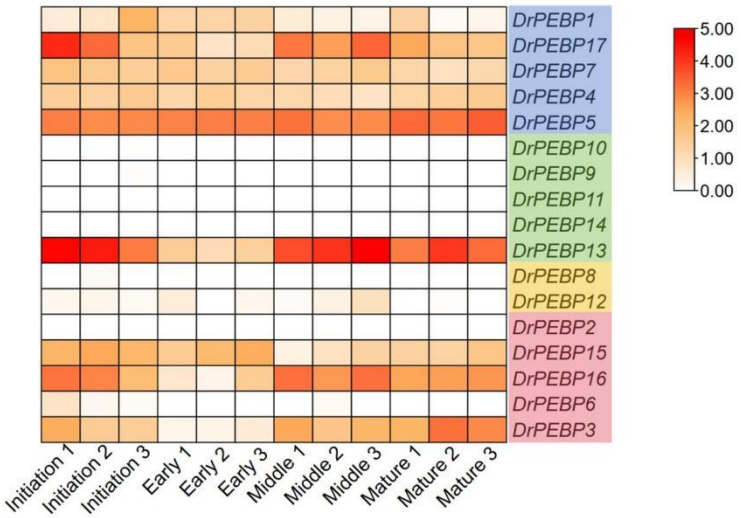


Fig. 7 Heatmap of *DrPEBP* expression levels. A. *DrPEBP* expression levels across 15 different tissues of yam. B. *DrPEBP* expression levels at various developmental stages of yam tubers. C. *DrPEBP* expression levels in healthy and scorch foot disease-affected yam plants. D. *DrPEBP* expression levels in healthy and wounded yam plants.

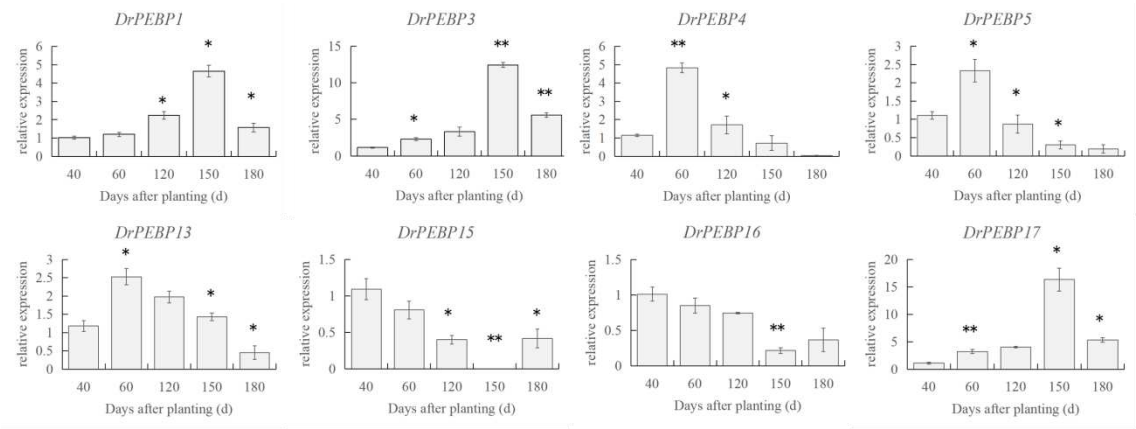
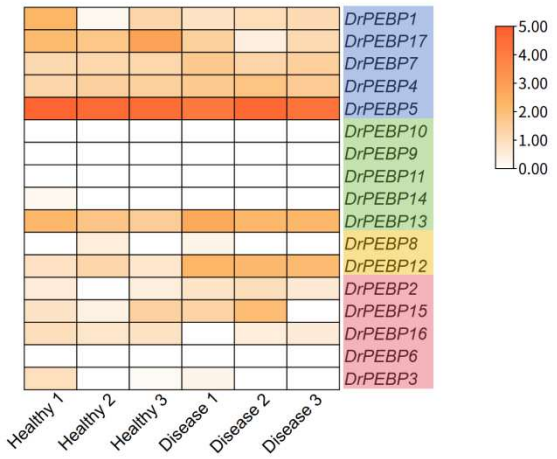


Fig. 8 The relative expression levels of nine selected *DrPEBPs* during the tuber expansion of yam. Values are presented as the mean ± standard deviation (SD) of three independent biological replicates. Asterisks indicate statistical significance compared to the previous stage, as determined by a two-tailed Student's t-test. Asterisks indicate statistical significance: ** $p<0.01$, and * $p<0.05$.

A



B

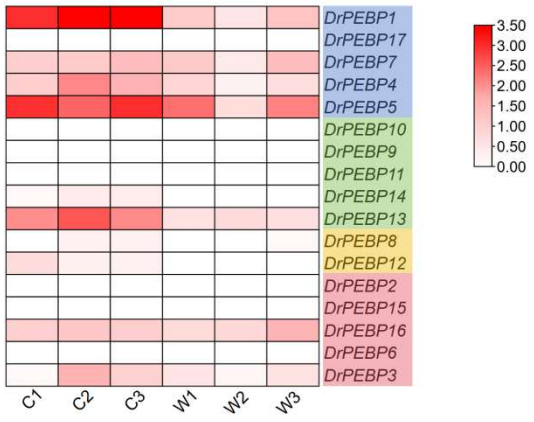


Fig. 9 *DrPEBP* expression levels in Response to Biotic and Abiotic Stresses. A. *DrPEBP* expression levels in healthy and scorch foot disease-affected yam plants. B. *DrPEBP* expression levels in healthy and wounded yam plants.

Author Contributions

Qiao Qinghua: Writing Original Draft, Conceptualization;

Gou Ling, Chen Meiling, Sheng Furui, and Gao Liujuan: Data analysis, manuscript review;

Ren Zhenxin: Conceptualization, supervision, Writing-Review and Editing.

All authors read and approved the final manuscript.

Acknowledgments

This work was supported by the National Natural Science Foundation of China (Grant No.32460770); Scientific Research Foundation of Yulin Normal University for high-level talents (Grant No. G2024ZK07).

Data Availability

Publicly available datasets were analyzed in this study. These datasets analyzed can be found in the NCBI SRA under accession numbers DRP003729 (https://trace.ncbi.nlm.nih.gov/Traces/?view=study&acc=DRP003729), SRP186810 (https://trace.ncbi.nlm.nih.gov/Traces/?view=study&acc=SRP186810), SRP298405 (https://trace.ncbi.nlm.nih.gov/Traces/?view=study&acc=SRP298405), SRP445455 (https://trace.ncbi.nlm.nih.gov/Traces/?view=study&acc=SRP445455) and SRP152752 (https://trace.ncbi.nlm.nih.gov/Traces/?view=study&acc=SRP152752).

Declarations

Conflict of Interests The authors declare that the research was conducted in the absence of any commercial, financial, or non-financial relationships that could be construed as a potential conflict of interest.

Reference

Abelenda JA, Bergonzi S, Oortwijn M, Sonnewald S, Du M, et al. 2019. Source-sink regulation is mediated by interaction of an FT homolog with a SWEET protein in Potato. Current Biology. 29(7):1178-1186. https://doi.org/10.1016/j.cub.2019.02.018.

Abelenda José A, Cruz-Oró E, Franco-Zorrilla J, Prat S. 2016. Potato StCONSTANS-like1

suppresses storage organ formation by directly activating the FT-like StSP5G repressor. Current Biology. 26(7):872-881. https://doi.org/10.1016/j.cub.2016.01.066.

Ahn JH, Miller D, Winter VJ, Banfield MJ, Lee JH, et al. 2006. A divergent external loop confers antagonistic activity on floral regulators FT and TFL1. The EMBO Journal. 25(3):605-14. https://doi.org/10.1038/sj.emboj.7600950.

Bennett T, Dixon LE. 2021. Asymmetric expansions of FT and TFL1 lineages characterize differential evolution of the EuPEBP family in the major angiosperm lineages. BMC Biology. 19(1):181. https://doi.org/10.1186/s12915-021-01128-8.

Bowers JE, Chapman BA, Rong J, Paterson AH. 2003. Unravelling angiosperm genome evolution by phylogenetic analysis of chromosomal duplication events. Nature. 422(6930):433-438. https://doi.org/10.1038/nature01521.

Cao K, Cui L, Zhou X, Ye L, Zou Z, Deng S. 2016a. Four tomato FLOWERING LOCUS T-Like proteins act antagonistically to regulate floral initiation. Frontiers in Plant Science. 6:1213. https://doi.org/10.3389/fpls.2015.01213.

Cao Y, Han Y, Li D, Lin Y, Cai Y. 2016b. MYB Transcription Factors in Chinese Pear (*Pyrus bretschneideri* Rehd.): Genome-Wide Identification, Classification, and Expression Profiling during Fruit Development. Frontiers in Plant Science. 7:577. https://doi.org/10.3389/fpls.

Carle-Urioste JC, Brendel V, Walbot V. 1997. A combinatorial role for exon, intron and splice site sequences in splicing in maize. The Plant Journal. 11(6):1253-1263. https://doi.org/10.1046/j.1365-313x.1997.11061253.x.

Chardon F, Damerval C. 2005. Phylogenomic Analysis of the *PEBP* Gene Family in Cereals. Journal of Molecular Evolution. 61(5):579-590. https://doi.org/10.1007/s00239-004-0179-4.

Cristina Sánchez-Rodas Navarro, Eduard Cruz-Oró, Prat S. 2015. Conserved function of FLOWERING LOCUS T (FT) homologues as signals for storage organ differentiation. Plant Biology. 23:45-53. https://doi.org/10.1016/j.pbi.2014.10.008.

Danilevskaya ON, Meng X, Hou Z, Evgueni Ananiev, Simmons CR. 2008. A Genomic and expression compendium of the expanded *PEBP* gene family from Maize. Plant Physiology. 146(1):250-264. https://doi.org/10.1104/pp.107.109538.

553 Dong L, Lu Y, Liu S. 2020. Genome-wide member identification, phylogeny and expression
554 analysis of *PEBP* gene family in wheat and its progenitors. PeerJ. 8:e10483-83.
555 https://doi.org/10.7717/peerj.10483.
556 Fernández-Nohales P, Domenech MJ, Martínez de Alba AE, Micol JL, Ponce MR, Madueño
557 F. 2014. AGO1 controls *Arabidopsis* inflorescence architecture possibly by regulating
558 TFL1 expression. Annals of Botany. 114(7):1471-1481.
559 https://doi.org/10.1093/aob/mcu132.
560 Fu C, Zhao M, Xia H, Ren P, Liu W, et al. 2025. Genome-wide identification and functional
561 analysis of the *PEBP* gene family in Begonia semperflorens “Super Olympia” reveal its
562 potential role in regulating flowering. International Journal of Molecular Sciences.
563 26(13):6291. https://doi.org/10.3390/ijms26136291.
564 Hanzawa Y, Money T, Bradley D. 2005. A single amino acid converts a repressor to an
565 activator of flowering. Proceedings of the National Academy of Sciences.
566 102(21):7748-7753. https://doi.org/10.1073/pnas.0500932102.
567 He J, Gu L, Tan Q, Wang Y, Hui F, et al. 2022. Genome-wide analysis and identification of
568 the *PEBP* genes of *Brassica juncea* var. Tumida. BMC Genomics. 23(1):535-535.
569 https://doi.org/10.1186/s12864-022-08767-3.
570 Hedman H, Källman T, Lagercrantz U. 2009. Early evolution of the MFT-like gene family in
571 plants. Plant Molecular Biology. 70(4):359-369.
572 https://doi.org/10.1007/s11103-009-9478-x.
573 Jeong S, Clark SE. 2004. Photoperiod regulates flower meristem development in *Arabidopsis*
574 *thaliana*. Genetics. 169(2):907-15. https://doi.org/10.1534/genetics.104.033357.
575 Jiang Y, Zhu Y, Peng Z, Su W, Peng J, et al. 2025. Two *FT* genes synergistically regulate the
576 reproductive transition of loquat. Horticultural Plant Journal. 11(2):548-563.
577 https://doi.org/10.1016/j.hpj.2023.08.003.
578 Jing S, Jiang P, Sun X, Yu L, Wang E, et al. 2023. Long-distance control of potato storage
579 organ formation by SELF PRUNING 3D and FLOWERING LOCUS T-like 1. Plant
580 Communications. 4(3):100547. https://doi.org/10.1016/j.xplc.2023.100547.
581 Kaneko-Suzuki M, Kurihara-Ishikawa R, Okushita-Terakawa C, Kojima C, Nagano-Fujiwara
582 M, et al. 2018. TFL1-Like proteins in rice antagonize rice FT-Like protein in

583 inflorescence development by competition for complex formation with 14-3-3 and FD.
584 Plant and Cell Physiology. 59(3):458-468. https://doi.org/10.1093/pcp/pcy021.
585 Karlgren A, Gyllenstrand N, Källman T, Sundström JF, Moore D, et al. 2011. Evolution of the
586 *PEBP* gene family in plants: functional diversification in seed plant evolution. Plant
587 Physiology. 156(4):1967-1977. https://doi.org/10.1104/pp.111.176206.
588 Khol M, Ma F, Lei L, Liu W, Liu X. 2024. A frontier review of nutraceutical Chinese yam.
589 Foods. 13(10):1426. https://doi.org/10.3390/foods13101426.
590 Kim G, Rim Y, Cho H, Hyun TK. 2022. Identification and functional characterization of
591 FLOWERING LOCUS T in platycodon grandiflorus. Plants. 11(3):325.
592 https://doi.org/10.3390/plants11030325.
593 Komiya R, Ikegami A, Tamaki S, Yokoi S, Shimamoto K. 2008. Hd3a and RFT1 are essential
594 for flowering in rice. Development. 135(4):767-74. https://doi.org/10.1242/dev.008631.
595 Kozlowski LP. 2021. Proteome-pI 2.0: proteome isoelectric point database update. Nucleic
596 Acids Research, 50: 1535-1540. https://doi.org/10.1093/nar/gkab944.
597 Lee R, Baldwin S, Kenel F, McCallum J, Macknight R. 2013. FLOWERING LOCUS T genes
598 control onion bulb formation and flowering. Nature Communications. 4(1):2884.
599 https://doi.org/10.1038/ncomms3884.
600 Li Y, Ren H, Zhang Y, Li R, Ai H, Huang X. 2022. Analysis of the molecular evolution of the
601 *PEBP* gene family in cruciferous plants. Biodiversity Science. 30(6):21545.
602 https://doi.org/10.17520/biods.2021545.
603 Lynch M. 2000. The evolutionary fate and consequences of duplicate genes. Science.
604 290(5494):1151-1155. https://doi.org/10.1126/science.290.5494.1151.
605 Manoharan R, Han J, Vijayakumar H, Subramani B, Thamilarasan S, et al. 2016. Molecular
606 and functional characterization of FLOWERING LOCUS T homologs in *Allium cepa*.
607 Molecules. 21(2):217. https://doi.org/10.3390/molecules21020217.
608 Mattick JS, Gagen MJ. 2001. The evolution of controlled multitasked gene networks: the role
609 of introns and other noncoding RNAs in the development of complex organisms.
610 Molecular Biology and Evolution. 18(9):1611-1630.
611 https://doi.org/10.1093/oxfordjournals.molbev.a003951.
612 Mohanta TK, Khan A, Hashem A, Abd_Allah EF, Al-Harrasi A. 2019. The molecular mass

and isoelectric point of plant proteomes. BMC Genomics. 20:631. https://doi.org/10.1186/s12864-019-5983-8.

Morris WL, M. Carmen Alamar, López-Cobollo R, Javier Castillo Cañete, Bennett MH, et al. 2018. A member of the TERMINAL FLOWER 1/CENTRORADIALIS gene family controls sprout growth in potato tubers. Journal of Experimental Botany. 70(3):835-843. https://doi.org/10.1093/jxb/ery387.

Munevver Dogramaci, Dobry EP, Fortini E, Fortini E, Sarkar D, et al. 2024. Physiological and molecular mechanisms associated with Potato tuber dormancy. Journal of experimental botany. 75(19):6093-6019. https://doi.org/10.1093/jxb/erae182.

Nakano Y, Higuchi Y, Sumitomo K, Hisamatsu T. 2013. Flowering retardation by high temperature in chrysanthemums: involvement of FLOWERING LOCUS T-like 3 gene repression. Journal of Experimental Botany. 64(4):909-920. https://doi.org/10.1093/jxb/ers370.

Nakano Y, Takase T, Katsuhiko Sumitomo, Suzuki S, Kana Tsuda-Kawamura, Tamotsu Hisamatsu. 2020. Delay of flowering at high temperature in Chrysanthemum: duration of darkness and transitions in lighting determine daily peak heat sensitivity. The Horticulture Journal. 89(5):602-608. https://doi.org/10.2503/hortj.utd-192.

Navarro C, Abelenda JA, Cruz-Oró E, Cuéllar CA, Tamaki S, et al. 2011. Control of flowering and storage organ formation in potato by FLOWERING LOCUS T. Nature. 478(7367):119-22. https://doi.org/10.1038/nature10431.

Nie M, Li L, He C, Lu J, Guo H, et al. 2024. Genome-wide identification, subcellular localization, and expression analysis of the phosphatidyl ethanolamine-binding protein family reveals the candidates involved in flowering and yield regulation of tartary buckwheat (*Fagopyrum tataricum*). PeerJ. 12:e17183. https://doi.org/10.7717/peerj.17183.

Padhan B, Panda D. 2020. Potential of neglected and underutilized yams (*Dioscorea* spp.) for improving nutritional security and health benefits. Frontiers in Pharmacology. 11:469. https://doi.org/10.3389/fphar.2020.00496.

Qiao Q, Li W, Li C, Zhou Y, Qiao W, et al. 2025.Genome-wide identification and expression analysis of the CrRLK1L gene family in yam (*Dioscorea rotundata*): potential roles in

643 growth and tuber development. Tropical Plant Biology. 18:4.
644 https://doi.org/10.1007/s12042-025-09409-0.
645 Qiao X, Li Q, Yin H, Qi K, Li L, et al. 2019. Gene duplication and evolution in recurring
646 polyploidization-diploidization cycles in plants. Genome Biology. 20:38.
647 https://doi.org/10.1186/s13059-019-1650-2.
648 Schwartz S, Meshorer E, Ast G. 2009. Chromatin organization marks exon-intron structure.
649 Nature Structural & Molecular Biology. 16(9):990-995.
650 https://doi.org/10.1038/nsmb.1659.
651 Sun C, Fang J, Zhao T, Xu B, Zhang F, et al. 2012. The histone methyltransferase SDG724
652 mediates H3K36me2/3 deposition at MADS50 and RFT1 and promotes flowering in rice.
653 The Plant Cell. 24(8):3235-3247. https://doi.org/10.1105/tpc.112.101436.
654 Sun Y, Jia X, Yang Z, Fu Q, Yang H, Xu X. 2023. Genome-wide identification of *PEBP* gene
655 family in *Solanum lycopersicum*. International Journal of Molecular Sciences.
656 24(11):9185. https://doi.org/10.3390/ijms24119185.
657 Tian Y, Wang J, Wang X, Wang D, Wang X, et al. 2025. Genome-wide identification,
658 phylogeny, and expression analysis of *PEBP* gene family in *Castanea mollissima*.
659 Frontiers in Genetics. 16:1530910. https://doi.org/10.3389/fgene.2025.1530910.
660 Vaistij FE, Barros-Galvão T, Cole AF, Gilday AD, He Z, et al. 2018.
661 MOTHER-OF-FT-AND-TFL1 represses seed germination under far-red light by
662 modulating phytohormone responses in *Arabidopsis thaliana*. Proceedings of the
663 National Academy of Sciences. 115(33):8442-8447.
664 https://doi.org/10.1073/pnas.1301647110.
665 Vaistij FE, Gan Y, Penfield S, Gilday AD, Dave A, et al. 2013. Differential control of seed
666 primary dormancy in *Arabidopsis* ecotypes by the transcription factor SPATULA.
667 Proceedings of the National Academy of Sciences of the United States of America.
668 110(26):10866-10871. https://doi.org/10.1073/pnas.1806460115.
669 Viruel J, Segarra-Moragues JG, Raz L, Forest F, Wilkin P, et al. 2015. Late Cretaceous-early
670 eocene origin of yams (*Dioscorea*, *Dioscoreaceae*) in the Laurasian Palaearctic and their
671 subsequent Oligocene-miocene diversification. Journal of Biogeography. 43(4):750-762.
672 https://doi.org/10.1111/jbi.12678.

673 Vision TJ, Brown DG, Tanksley SD. 2000. The origins of genomic duplications in
674 *Arabidopsis*. Science. 290(5499):2114-2117.
675 https://doi.org/10.1126/science.290.5499.2114.
676 Wang Q, Zhou Y, Wang F, Li X, Yu Y, et al. 2025. Genome-wide identification of *PEBP* gene
677 family in *Hedychium coronarium*. Frontiers in Plant Science. 16:1482764.
678 https://doi.org/10.3389/fpls.2025.1482764.
679 Xi W, Liu C, Hou X, Yu H. 2010. MOTHER OF FT AND TFL1 regulates seed germination
680 through a negative feedback loop modulating ABA signaling in *Arabidopsis*. The Plant
681 Cell. 22(6):1733-1748. https://doi.org/10.1105/tpc.109.073072.
682 Xiang Jia Min, Powell BA, Braessler J, Meinken J, Yu F, Gaurav Sablok. 2015. Genome-wide
683 cataloging and analysis of alternatively spliced genes in cereal crops. BMC Genomics.
684 16(1):721. https://doi.org/10.1186/s12864-015-1914-5.
685 Xu H, Guo X, Hao Y, Lu G, Li D, et al. 2022. Genome-wide characterization of *PEBP* gene
686 family in *Perilla frutescen*s and *PfFT1* promotes flowering time in *Arabidopsis thaliana*.
687 Frontiers in Plant Science. 13:1026696. https://doi.org/10.3389/fpls.2022.1026696.
688 Yang J, Ning C, Liu Z, Zheng C, Mao Y, et al. 2023. Genome-wide characterization of *PEBP*
689 gene family and functional analysis of TERMINAL FLOWER 1 homologs in
690 *Macadamia integrifolia*. Plants. 12(14):2692-2692.
691 https://doi.org/10.3390/plants12142692.
692 Yu X, Liu H, Sang N, Li Y, Zhang T, et al. 2019. Identification of cotton MOTHER OF FT
693 AND TFL1 homologs, GhMFT1 and GhMFT2, involved in seed germination. PLoS
694 ONE. 14(4):e0215771. https://doi.org/10.1371/journal.pone.0215771.
695 Zhang G, Jin X, Li X, Zhang N, Li S, et al. 2022. Genome-wide identification of *PEBP* gene
696 family members in potato, their phylogenetic relationships, and expression patterns
697 under heat stress. Molecular Biology Reports. 49(6):4683-4697.
698 https://doi.org/10.1007/s11033-022-07318-z.
699 Zhang X, Campbell R, Laurence, Morris J, Hedley PE, et al. 2020. TERMINAL
700 FLOWER-1/CENTRORADIALIS inhibits tuberisation via protein interaction with the
701 tuberigen activation complex. The Plant Journal. 103(6):2263-2278.
702 https://doi.org/10.3389/fpls.2023.1277436.

Zhang X, Ouyang Y, Zhao L, Li Z, Zhang H, Wei Y. 2023. Genome-wide identification of *PEBP* gene family in pineapple reveal its potential functions in flowering. Frontiers in Plant Science. 14:1277436. https://doi.org/10.1371/journal.pone.0161080.

Zhang X, Wang C, Pang C, Wei H, Wang H, et al. 2016. Characterization and functional analysis of *PEBP* family genes in upland cotton (*Gossypium hirsutum* L.). PLoS ONE. 11(8):e0161080. https://doi.org/10.1111/tpj.14898.

Supplementary Files

This is a list of supplementary files associated with this preprint. Click to download.

- SupplementaryTable.xlsx
- SupplementaryFig1.jpg
- SupplementaryFig2.jpg